PROCEEDINGS OF SCIENCE

Galactic cosmic ray quiet time spectra from 300 MeV up to above 1 GeV measured with SOHO/EPHIN

Kühl, P.*, Dresing, N., Gieseler, J., Heber, B., Klassen, A.
IEAP, University of Kiel, 24098 Kiel, Germany
E-mail: kuehl@physik.uni-kiel.de

The solar modulation of galactic cosmic rays (GCR) can be studied in detail by long term variations of the GCR energy spectrum (e.g. on the scales of a solar cycle). With almost 20 years of data, the Electron Proton Helium INstrument (EPHIN) aboard SOHO is well suited for these kind of investigations. Although the design of the instrument is optimized to measure proton and helium isotope spectra up to 50 MeV/nucleon the capability exists that allow to determine energy spectra up to above 300 MeV/nucleon. Therefore we developed a sophisticated inversion method to calculate such proton spectra. The method relies on a GEANT4 Monte Carlo simulation of the instrument and a simplified spacecraft model that calculates the energy response function of EPHIN for electrons, protons and heavier ions. In order to determine the energy spectra the resulting inversion problem is solved numerically. As a result we present galactic cosmic ray spectra from 2006-2009. For validation, the derived spectra are compared to those determined by the PAMELA instrument.

The 34th International Cosmic Ray Conference,
30 July- 6 August, 2015
The Hague, The Netherlands

*Speaker.

PoS(ICRC2015)224

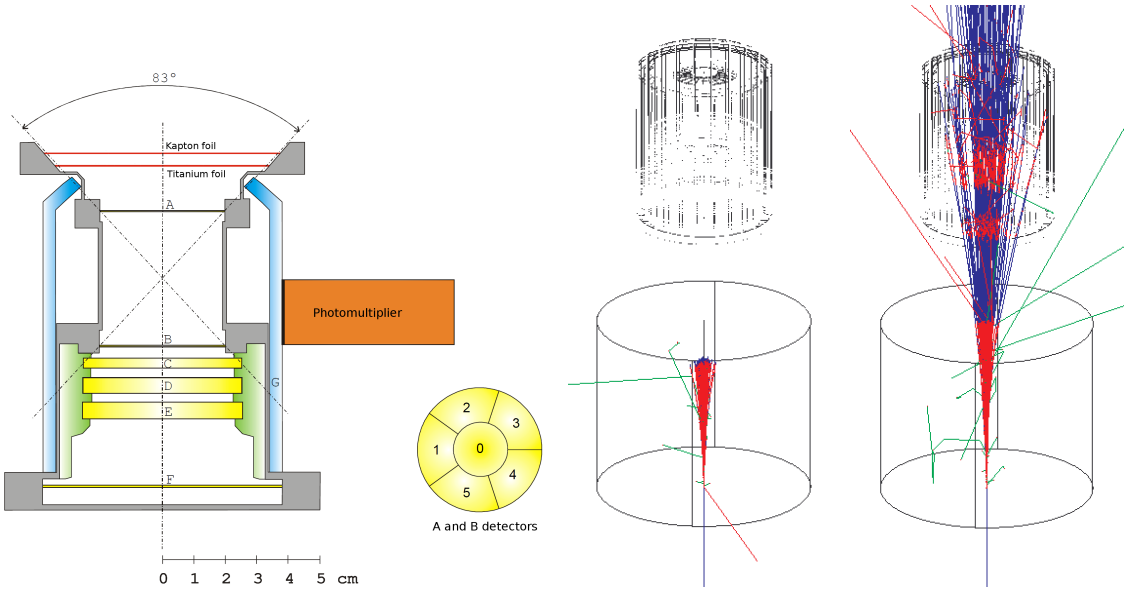

Figure 1: Sketch of the EPHIN instrument [Müller-Mellin et al. (1995)] and the instrument as implemented in the GEANT4 simulation including a 10 cm block of aluminium to mimic the spacecraft. Simulated trajectories of a 150 MeV (center) and 200 MeV (right) proton beam including secondary particles created in the shielding are also shown. The colors represent the particle-type, protons (red), electrons (blue) and gammas (green).

1. Introduction

The intensity of galactic cosmic rays (GCR) in the inner heliosphere is well known to vary on time-scales of eleven years, anti-correlated to the solar activity cycle. This modulation of the GCR particles can be described by convection in the solar wind, adiabatic cooling, diffusion and drift effects [Parker (1965)], with the latter one also depending on the alignment of the interplanetary magnetic field and hence on the 22-year cycle of the solar dynamo. To investigate these drift effects, which are often neglected in models such as the force-field solution [Gleeson & Axford (1968)], long-term measurements of the GCR spectrum at energies of several hundreds of MeV are needed. In this work, we show that the Electron Proton Helium Instrument (EPHIN, [Müller-Mellin et al. (1995)]) aboard the Solar and Heliospheric Observatory (SOHO) with its mission life-time of almost 20 years is well suited for these kind of analysis. While the nominal maximum energy at which the instrument can determine spectra for protons is $\approx 50\ MeV$, a simple yet sophisticated inversion method based on GEANT4 simulations [GEANT4 Collaboration (2006)] can be used to derive proton energy spectra in the range between 100 MeV and 1 GeV during solar events [Kühl et al. (2015)]. However, in comparison to solar events, the GCR spectrum features a different spectral shape as well as different fluxes of electrons and helium particles which may corrupt the measurements. Thus, we will discuss the capabilities, limitations and systematic uncertancies of this method. Furthermore, preliminary results of the GCR spectra at several hundreds of MeV based on EPHIN data from 2006 to 2009 are presented in comparison to PAMELA data [Adriani et al. (2013)].

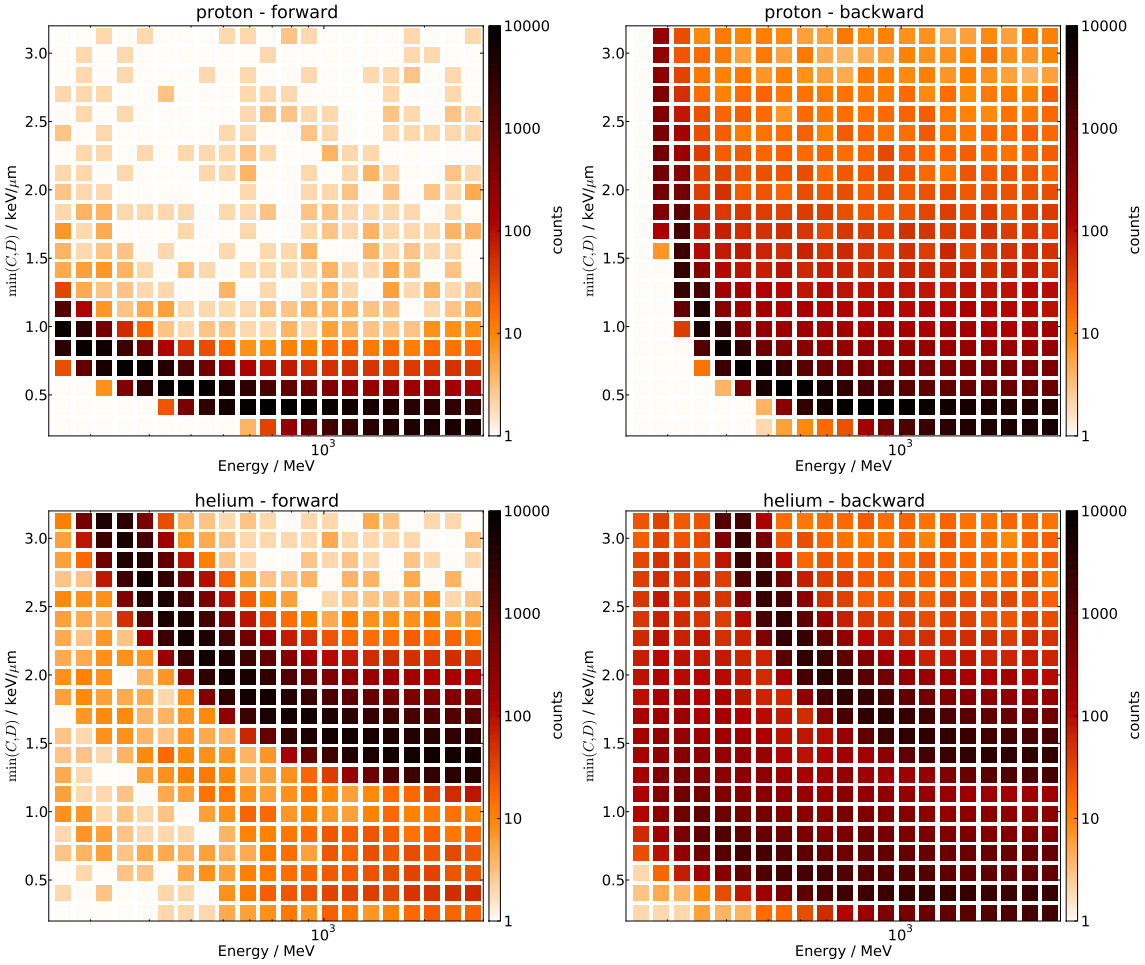

Figure 2: Simulation results for isotropic fluxes of protons (upper row) and helium particles (lower row) in front of (left column) and behind the instrument (right column). For each mono-energetic simulation (horizontal axis), a histogram of the resulting energy losses is shown color-coded.

2. Instrumentation and Inversion Method

A sketch of the EPHIN instrument is shown in fig. 1 (left). The instrument consists of a stack of silicon solid state detectors (SSDs, A-F) surrounded by an anticoincidence (scintilator, G). In this work, we focus on high energy particles that penetrate the entire instrument and deposit energy in every SSD. Since no information of the directionality of the measured particles is known, one can not simply distinguish between particles entering the instrument from the front ("forward particles", entering at detector A, exiting at detector F) and particles entering the instrument from behind ("backward particles", entering at detector F, exiting at detector A). Since backward particles first have to penetrate the entire spacecraft, they will reach the actual instrument with only a fraction of their initial energy which leads to systematic uncertancies in the derived spectra (c.f. [Kühl et al. (2015)] for details). To take this effects into account, a GEANT4 simulation has been set up, including a 10 cm aluminium block behind the instrument to mimic the spacecraft shielding as shown in fig. 1. In addition, the figure includes trajectories of simulated proton beams with

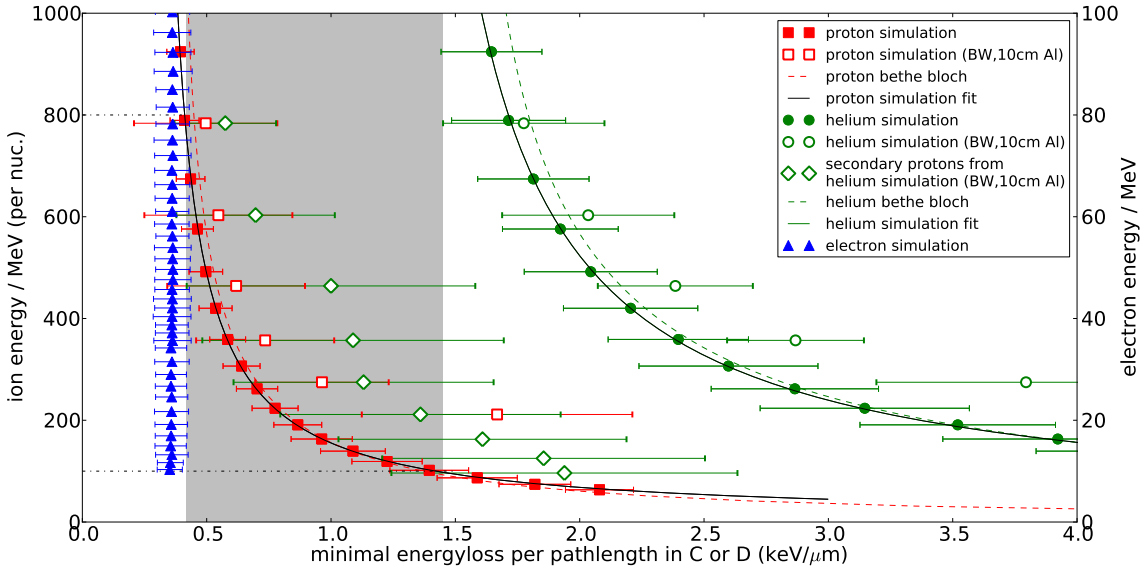

Figure 3: Relation between initial total energy and energy loss in the detector for protons (red), helium particles (green) and electrons (blue, right hand axis). The maximum energy of electrons is chosen to be 100 MeV based on measurements [Moses et al. (1989)]. Open symbols represent results from backward simulations, secondary protons caused by helium (green diamonds) are shown individually.

150 MeV and 200 MeV (center, right). The trajectories indicate that a backward proton needs to have an energy of roughly 150-200 MeV to penetrate both the shielding as well as all six SSDs. Hence, the energy response for forward particles (which need to have $\approx$ 50 MeV to penetrate the detector) differs from the response for backward particles, especially at lower energies.

To calculate the initial total energy of a penetrating particle based on the energy deposition in the detector, mono-energetic simulations with isotropic fluxes of protons, electrons and helium particles in front of (for forward particles) and behind the instrument (backward particles) have been performed individually. Results for protons and helium particles are shown in fig. 2. The figure shows the resulting counts (color-coded) as a function of the energy-loss and the initial total energy. For the energy loss, the minimum of the energy deposition in either the C or D detector is used to reduce noise based on the statistical nature of the energy loss (c.f. [Kühl et al. (2015)]). For both, protons and helium particles, the forward particles form a narrow population with a clear relation between total energy and energy loss, as expected based on the Bethe-Bloch equation. The backward particles on the other hand can cause a wide variety of energy losses due to the interaction in the spacecraft. Furthermore, at low energies the energy loss is enhanced as backward particles at this energies loose a significant fraction of their energy in the shielding. In addition, the distribution of backward helium particles shows a secondary population at typical energy losses of protons, which are caused by secondary protons created in the shielding via nuclear interactions.

To quantify the relation between energy loss and total energy, the simulation results are summed up in fig. 3, where the initial energy is plotted as a function of the mean energy loss. Results for electrons (blue), protons (red) and helium (green) are shown individually. Backward and forward results are represented by filled and open symbols, respectively. The secondary protons caused by interaction of backward helium in the spacecraft are also shown (green diamonds). From the figure

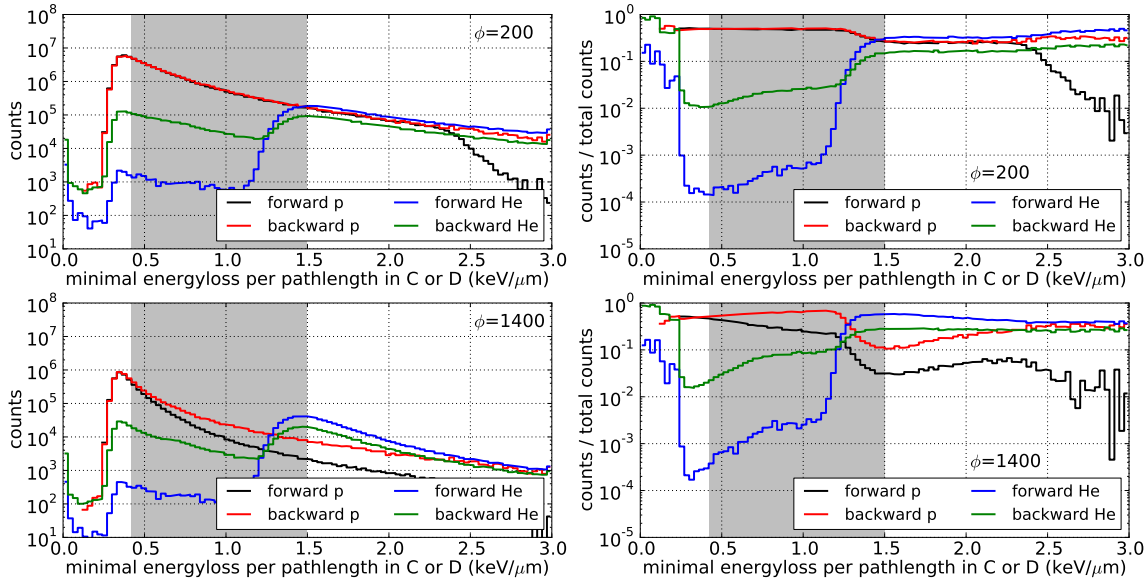

Figure 4: Expected counts (left: total counts, right: normalized counts) as function of energy loss for protons and helium particles entering the instrument from front and behind. Upper row shows results for solar minimum (ϕ=200 MV), lower row for solar maximum (ϕ=1400 MV).

it is clear that 1) energy deposition caused by electrons is limited to $\approx$ 0.4 keV/μm; 2) helium causes energy depositions above $\approx$ 1.4 keV/μm (except for secondary protons created by helium interacting in the spacecraft); and 3) that energy losses in the intermediate region (gray shaded in the figure) are almost entirely caused by protons. Furthermore, forward protons can be easily described by an analytic fit (red dashed line) and therefore, measured energy losses between 0.4 and 1.4 keV/μm can be converted into a proton spectrum with energies from $\approx$ 150 MeV up to over 1 GeV.

Note that energies below 150 MeV are corrupted by helium particles that have energy losses similar to low energy protons (c.f. fig. 3) which results in overestimated fluxes. Furthermore, measured spectra can have a small background of helium contribution in general in any energy bin. To address this issue, the amount of counted particles is estimated. Using the force-field solution [Gleeson & Axford (1968), Usoskin et al. (2011)], the energy spectra based on the particle type and the solar modulation (i.e. the solar modulation potential ϕ) is approximated. These spectra are then used as input for the GEANT4 simulation. The resulting number of particles counted in the simulations are shown in fig. 4 for both forward and backward penetrating particles during both, solar minimum (ϕ=200 MV) and solar maximum (ϕ=1400 MV). From the figure, it is obvious that the number of counts with energy losses below $\approx$ 1.2 keV/μm caused by helium particles is of the order of serveral % under both solar activity conditions and hence, the helium corruption above $\approx$ 150 MeV can be neglected.

In addition to the helium corruption, another systematic error is caused by backward penetrating protons. Fig. 3 indicates that the fit used to calculate the initial energy based on the energy loss deviates from the simulation results of the backward protons. The deviation increases to lower energies (especially below $\approx$ 300 MeV), while both datasets converge at higher energies.

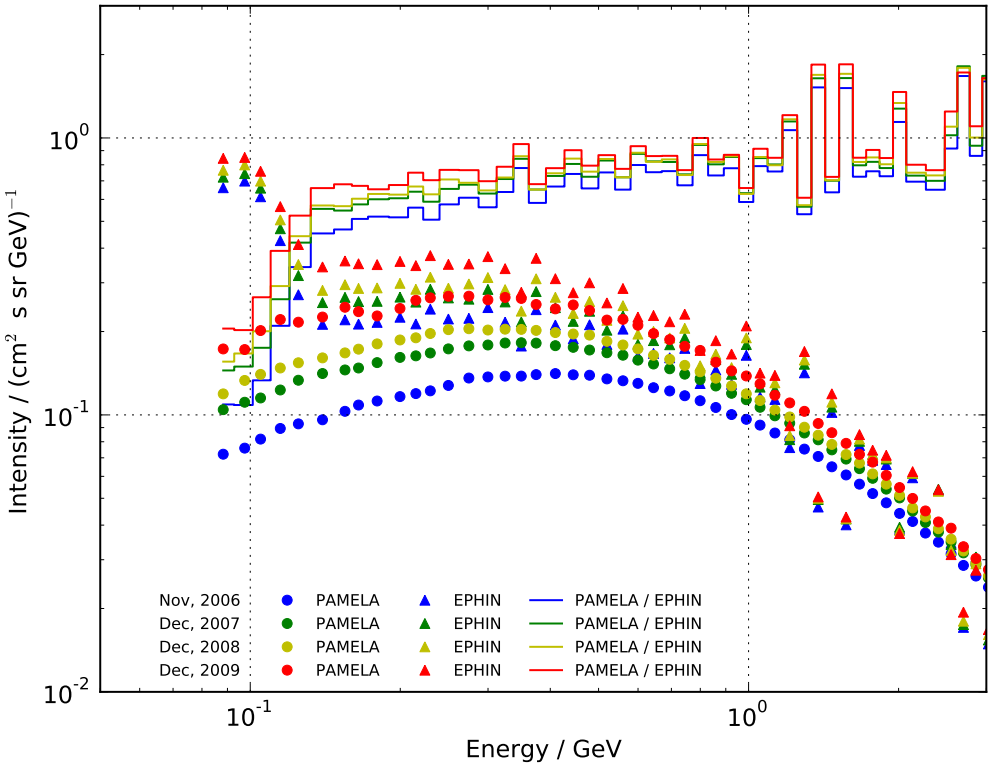

Figure 5: Proton spectra from 2006 to 2009, results from this work based on EPHIN data (triangles) in comparison to PAMELA results (circles, [Adriani et al. (2013)]). The solid lines indicate the ratio of both measurements.

Hence, unless a more sophisticated numerical inversion method is applied [Böhm et al. (2007), Köhler et al. (2011)], the presented method is limited to energies above $\approx$ 300 MeV for galactic cosmic ray spectra.

3. Results and Discussion

The presented method was applied to EPHIN data of four different time-periods (Nov 2006, Dec 2007, Dec 2008 and Dec 2009). The time-periods are chosen to cover several years in order to investigate the variation of the GCR spectra due to solar modulation. Furthermore, comparable PAMELA data is required to be available for validation. The resulting spectra are shown in fig. 5 in comparison to PAMELA data [Adriani et al. (2013)]. The solid lines represent the intensity ratio of both instruments.

Below $\approx$ 150 MeV the EPHIN spectra features an increased flux, roughly one order of magnitude higher than the PAMELA data. The increased fluxes show almost no variation over the the four years, indicating that the measured particles should have a high rigidity. Hence, in agreement to section 2, these particles can be identified as high energy helium particles that corrupt the proton spectra at these energies.

However, the energy range from $\approx$ 300 MeV up to $>$ 1 GeV is in good agreement to the PAMELA data. While a general offset (EPHIN fluxes are 10-20% larger than PAMELA fluxes) occours, no systematic time- or energy-dependent deviations are found. Note that the variations above 1 GeV are of statistical nature due to the fine binning which was chosen in order to allow direct comparison with the PAMELA data.
In the intermediate energy-range (150-300 MeV), a clear trend with decreasing quality of the EPHIN data towards lower energies can be observed. The ratio indicates that the quality varies with the solar cycle and hence the overall shape of the GCR spectrum. In agreement to section 2, this effect can be identified to be caused by backward protons and the systematic error in the calculation of their total energy.

We conclude that using a simple yet sophisticated inversion method, SOHO/EPHIN is capable of measuring the galactic cosmic ray proton quiet time spectra in the energy range from $\approx$ 300 MeV up to over 1 GeV. However, for lower energies (e.g. 150-300 MeV) a more complex analysis of the instrument and its data is necessary.

Acknowledgments

We are grateful to the PAMELA team for making their data publicly available. The SOHO/EPHIN project is supported under Grant 50 OC 1302 by the German Bundesministerium für Wirtschaft through the Deutsches Zentrum für Luft- und Raumfahrt (DLR). This project has received funding from the European Unions Horizon 2020 research and innovation programme under grant agreement No 637324.

References

[Adriani et al. (2013)] Adriani, O. et al., 2013, APJ, 765, 91

[Böhm et al. (2007)] Böhm, E., Kharytonov, A. & Wimmer-Schweingruber, R. F. 2007, A&A, 473, 673-682

[GEANT4 Collaboration (2006)] GEANT4 Collaboration 2006, CERN-LHCC 98-44, see also: http://geant4.cern.ch/

[Gleeson & Axford (1968)] Gleeson, L. J. & Axford, W. I., 1968, APJ, 154, 1011

[Köhler et al. (2011)] Köhler, J. et al., 2011, NIMP, 269, 2641-2648

[Parker (1965)] Parker, E., 1965, Planet. Space Sci., 13:9âĂŞ49

[Usoskin et al. (2011)] Usoskin, I. G. and Bazilevskaya, G. A. and Kovaltsov, G. A., 2011, JGR, 116, 2104

[Kühl et al. (2015)] Kühl, P. et al., 2015, A&A, 576, 120

[Moses et al. (1989)] Moses, D., Droege, W., Meyer, P. & Evenson, P. 1989, ApJ, 346, 52

[Müller-Mellin et al. (1995)] Müller-Mellin, R., Kunow, H., Fleissner, V., et al. 1995, Sol. Phys., 162, 483